The electron spin resonance and optical spectra of Ce^{3+} in $LiYF_4$

1997 J. Phys.: Condens. Matter 9 3733

(http://iopscience.iop.org/0953-8984/9/18/012)

J. Phys.: Condens. Matter **9** (1997) 3733–3739. Printed in the UK PII: S0953-8984(97)79600-0

The electron spin resonance and optical spectra of Ce^{3+} in $LiYF_4$

T Yosida†, M Yamaga‡, D Lee§, T P J Han§, H G Gallagher§ and B Henderson§

† Nakanihon Automotive College, Kamo, 505, Japan

‡ Department of Electronics, Faculty of Engineering, Gifu University, Gifu, 501-11, Japan

§ Department of Physics and Applied Physics, University of Strathclyde, Glasgow G1 1XN, UK

Received 15 November 1996

Abstract. The electron spin resonance (ESR) of Ce^{3+} in $LiYF_4$ was measured with an X-band frequency and low temperatures. The Ce^{3+} ions in this crystal show tetragonal symmetry with $g_{\parallel} = 2.765(2)$ and $g_{\perp} = 1.473(2)$. The analysis of the g-tensor indicates that the ground-state wavefunctions have dominant components of $|J, J_z\rangle = |5/2, \pm 5/2\rangle$, resulting in a negative value of the crystal-field parameter B_2^0. Three optical absorption bands with peaks at <210 nm, 248 nm, and 298 nm were observed at room temperature. The 298 nm band is more strongly polarized along the a-axis than along the c-axis, whereas the 248 nm band shows the reverse polarization. The properties of the polarization can be explained by using wavefunctions of the lower ^{2}E excited state of Ce^{3+}, which is split into $|x^2 - y^2\rangle$ and $|2z^2 - x^2 - y^2\rangle$ in tetragonal symmetry, $|x^2 - y^2\rangle$ being lower in energy.

1. Introduction

There is much current interest in Ce^{3+}-doped ionic crystals for potential applications in sensors [1–3] and in UV lasers [4, 5]. The Ce^{3+} ion in its lowest-energy state has a single 4f electron outside the closed shells. In consequence, the electronic ground state $^2F_{5/2}$ is separated by spin–orbit interaction from the lowest excited state $^2F_{7/2}$ by approximately 2000 cm^{-1}. The next higher configuration corresponds to the promotion of the 4f electron into the 5d orbital, some 30 000–40 000 cm^{-1} higher in energy. The 4f–5d transitions occur via allowed electric dipole processes which have large transition probabilities. Since the electron–phonon couplings of 4f and 5d electrons are quite different, the 4f–5d transitions feature broad absorption and emission bands with large Stokes shifts between them, giving rise to a wide tuning range of laser oscillation. Recently, the properties of an optically pumped solid-state UV tunable laser obtained from a Ce^{3+}-doped $LiYF_4$ crystal at room temperature were reported [5]. We examine the relationship between the high optical quality of the crystal required for laser performance and the environment of Ce^{3+} in the crystal. Electron spin resonance (ESR) reveals the local structure of rare-earth ions in crystals. This paper reports on the crystal growth of Ce^{3+}-doped $LiYF_4$ and its characterization by using ESR and polarized optical absorption spectra.

2. The crystal structure and experimental procedure

$LiYF_4$ exhibits scheelite structure, space group $I4_1/a$, as shown in figure 1, with the lattice constants $c = 10.94$ Å and $a = 5.26$ Å [6]. Each Li^+ ion is located at the centre of a

0953-8984/97/183733+07$19.50

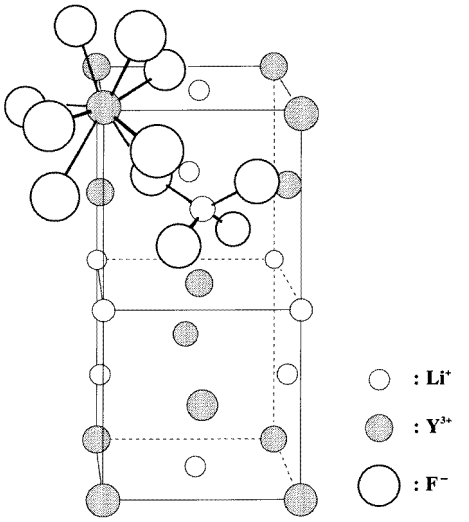

Figure 1. The crystal structure of $LiYF_4$.

regular tetrahedron of F^- ions, and the Y^{3+} ions are each surrounded by eight F^- ligands forming a tetragonal dodecahedron (S_4 symmetry). On the basis of the similar ionic radii and chemical properties of Ce^{3+} and Y^{3+} ions, Ce^{3+} is expected to substitute for Y^{3+}.

Single crystals of $LiYF_4$ nominally doped with 1 at.% Ce were grown by the vertical Bridgman–Stockbarger technique. The crystallization temperature is 819 °C. An atmosphere of purified flowing Ar gas was maintained in the chamber to prevent the progressive loss of LiF from the melt. The samples were cut and polished to approximate dimensions $2 \times 3 \times 5$ mm^3 and $0.4 \times 3 \times 5$ mm^3, the long dimension being parallel to the *c*-axis; these were used for ESR and optical measurements, respectively.

The ESR measurements were made using a Varian X-band spectrometer with 270 Hz field modulation. The cavity was immersed in liquid helium at 4.2 K. Temperatures above 4.2 K were controlled by a heater wound around the cavity; the evaporating He gas left liquid He at the bottom of the Dewar vessel. Sample temperatures were monitored using a thermocouple set near the sample. The absorption coefficient was measured using a Cary-AVIV double-beam spectrophotometer at 300 K and with the wavelength in the range 200–3500 nm. The polarized optical absorption was measured by placing a Glan–Taylor prism in the sample beam of the spectrophotometer.

3. Experimental results

3.1. ESR spectra

Figure 2 shows the ESR spectra measured at 4.2 K, with a microwave power of 0.02 mW and a microwave frequency of 9.328 GHz, with the magnetic field $\boldsymbol{B} \parallel \boldsymbol{c}$ and $\boldsymbol{a}$. The width of the strong ESR line for $\boldsymbol{B} \parallel \boldsymbol{c}$ or $\boldsymbol{a}$ is about 15 G, and fluorine hyperfine structures are barely observable. The ESR line does not split in any direction of magnetic field applied in the *a–c* plane and the resonance magnetic field remains constant in the *a–a* plane. The

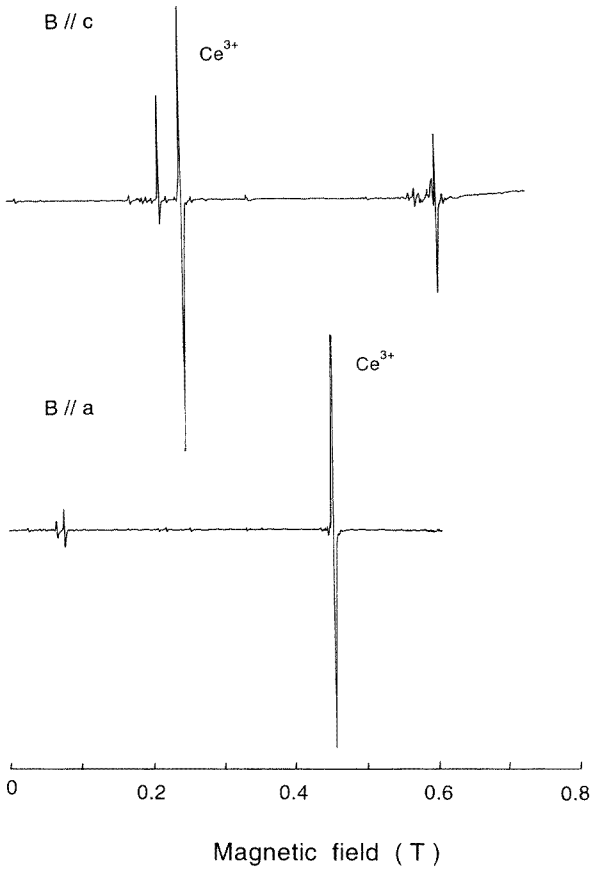

Figure 2. The ESR spectra of Ce^{3+} in $LiYF_4$ measured at 4.2 K, with a microwave frequency of 9.328 GHz, and with $\boldsymbol{B} \parallel \boldsymbol{c}$ and $\boldsymbol{a}$.

angular dependence of the ESR spectra may be fitted to the spin Hamiltonian

$$\mathcal{H} = \mu_B g_\parallel H_z S_z + \mu_B g_\perp (H_x S_x + H_y S_y) \tag{1}$$

with effective spin $S = 1/2$, where μ_B is the Bohr magneton. The principal z-, x- and y-axes are parallel to the crystal c-, a-, and b-axes, respectively. The g-values, estimated to be $g_\parallel = 2.765(2)$ and $g_\perp = 1.473(2)$, are very similar to those ($g_\parallel = 2.91$, $g_\perp = 1.42$) observed for Ce^{3+}:$CaWO_4$ [7, 8]. In consequence, the ESR lines are assigned to Ce^{3+}. The weak lines in figure 2 are interpreted as being due to unintentionally introduced impurity ions (Er^{3+} and Dy^{3+}, judging from their g-values [9]).

The peak-to-peak intensities of the ESR lines in figure 2 decrease rapidly with increasing temperature, to such an extent that they are not detected above 40 K as a consequence of the line broadening induced by spin–lattice interaction. Figure 3 shows the temperature dependence of the linewidth of the ESR line with $\boldsymbol{B} \parallel \boldsymbol{c}$ as a function of the inverse of the temperature T. The linewidth is defined as the peak-to-peak separation, Δ_{pp}, of the first derivative.

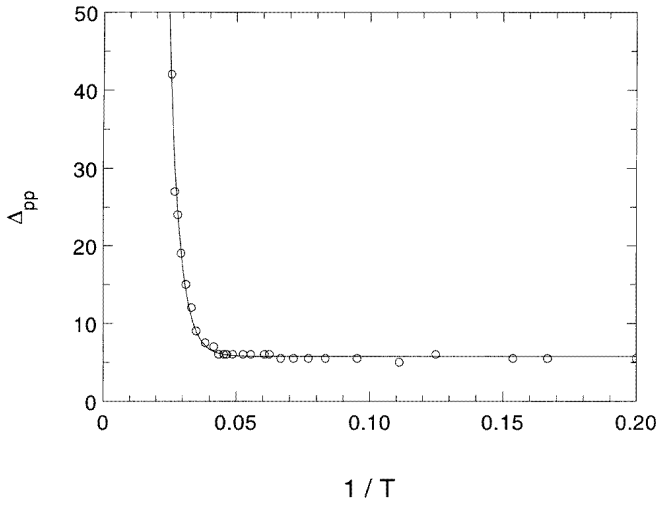

Figure 3. The linewidth of the ESR line for $\boldsymbol{B} \parallel \boldsymbol{c}$ versus $1/T$.

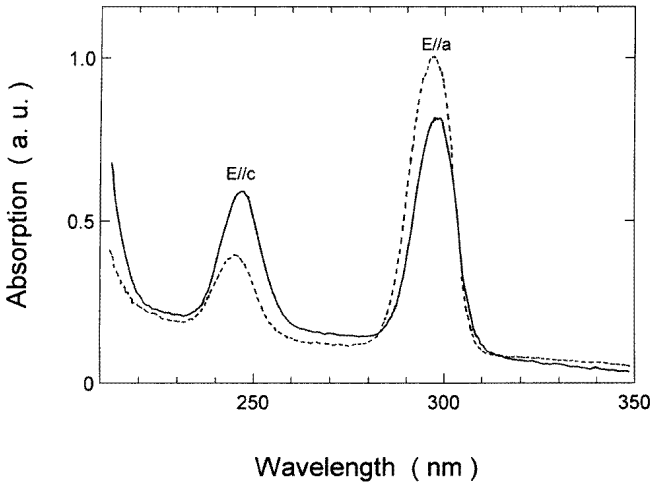

Figure 4. The polarization of the optical absorption of Ce^{3+} in $LiYF_4$ measured at 300 K.

3.2. Optical spectra

Figure 4 shows the polarized optical absorption spectra. Three absorption bands with peaks at <210 nm, 248 nm and 298 nm are observed at room temperature. The spectrum is very similar to that of Ce^{3+} in $LiYbF_4$, which is of the same crystal family as $LiYF_4$ [3]. These absorption bands correspond to the transition from the $^2F_{5/2}$ ground state to the excited states of Ce^{3+}. The 298 nm absorption band is more strongly polarized along the a-axis than along the c-axis—designated σ-polarization—whereas the 248 nm band is polarized along the c-axis about twice as strongly as along a-axis—designated π-polarization.

The luminescence spectrum excited at 280 nm and measured at room temperature shows double peaks at 310 nm and 324 nm, which are ascribed to the energy separation of $^2F_{5/2}$

and $^2F_{7/2}$, which is approximately 1400 cm^{-1}. Although the peak energies are the same as those in reference [5], the relative intensity of the two bands is slightly different from that in reference [5].

4. Discussion

4.1. The ground state and its splitting

The g-tensor of Ce^{3+} may be discussed in terms of the wavefunctions of the ground state. The $^2F_{5/2}$ ground state is split into three Kramers doublets by the crystal field. The crystal-field Hamiltonian for tetragonal symmetry (S_4) is

$$\mathcal{H}_{cry} = B_2^0 O_2^0 + B_4^0 O_4^0 + B_4^4 O_4^4 + B_6^0 O_6^0 + B_6^4 O_6^4 + B_6^6 O_6^6 \tag{2}$$

where the O_n^m are spin operators and the B_n^m are constants to be determined [10, 11]. The Hamiltonian including only the terms O_n^0 gives the eigenfunctions $|J, J_z\rangle = |5/2, \pm 1/2\rangle, |5/2, \pm 3/2\rangle, |5/2, \pm 5/2\rangle$, although their energy levels are determined by the magnitudes of B_n^0. The g-values calculated using the eigenfunction of these pure-spin states are not in agreement with the observed g-values [10, 11].

In order to resolve this discrepancy, the crystal-field term O_4^4 which mixes the spin state $|5/2, \mp 3/2\rangle$ into $|5/2, \pm 5/2\rangle$ must be considered. The g-value is then calculated by the same method as was followed for Ce^{3+} in the case of $CaWO_4$ [10]. The wavefunction of the ground state is assumed to be

$$\left|\frac{5}{2}, \pm\frac{5'}{2}\right\rangle = \cos\theta \left|\frac{5}{2}, \pm\frac{5}{2}\right\rangle + \sin\theta \left|\frac{5}{2}, \mp\frac{3}{2}\right\rangle \tag{3}$$

and the resulting g-values are

$$\begin{aligned} g_\parallel &= g_L(8\cos^2\theta - 3) \\ g_\perp &= g_L|2\sqrt{5}\cos\theta\sin\theta| \end{aligned} \tag{4}$$

where g_L (=6/7) is the Landé factor for $J = 5/2$.

The g-values ($g_\parallel = 2.774, g_\perp = 1.590$) calculated using equation (4) with $\theta = 28^\circ$ give a close fit to the experimental results ($g_\parallel = 2.765, g_\perp = 1.473$). The small difference may be explained by the admixture of the spin state $|7/2, \mp 7/2\rangle$ into $|5/2, \pm 5/2\rangle$ through the operator O_6^6 [10]. The fact that the ground-state wavefunctions have the components $|5/2, \pm 5/2\rangle$ dominant suggests that the diagonal matrix elements of $B_2^0 O_2^0$ and $B_4^0 O_4^0$ are much larger than the off-diagonal matrix element of $B_4^4 O_4^4$, and that the value of B_2^0 must be negative. This negativity of the value of B_2^0 implies that the tetragonal dodecahedron is compressed along the c-axis. This expectation is in agreement with the crystal-field parameters determined from the optical absorption and fluorescence spectra of Er^{3+} in $LiYF_4$ [12, 13].

The energy separation of the first excited state of $J = 5/2$ can be estimated from the spin–lattice relaxation time measurement for the ground state. The inverse of the relaxation time is proportional to the linewidth of the ESR line. Assuming that the Orbach process is dominant and taking into account the experimental result that the linewidth Δ_{pp} is nearly constant over the range 0.5–2 of $1/T$, the linewidth is given by

$$\Delta_{pp} = a + b\exp\left(-\frac{\Delta E}{kT}\right) \tag{5}$$

where a and b are constants independent of T, and ΔE is the energy separation between the ground and first excited states. The solid curve in figure 3, calculated using equation (5)

with $a = 5.8$, $b = 2.3 \times 10^4$ and $\Delta E = 175\ \mathrm{cm}^{-1}$, fits to the observed data. The value of the constant a suggests that the inhomogeneous linewidth that is independent of the temperature is much larger than the linewidth produced by the direct process, which is dominant at low temperatures. However, the ESR results give no information about the wavefunction of the first excited state nor about the energy level and wavefunction of the second excited state. An infrared absorption measurement is required to clarify the energy level structure of $^2F_{5/2}$ of Ce^{3+} in $LiYF_4$.

4.2. The excited state and its splitting

The ESR results indicate that the ^2F_J ground state is first split by the spin–orbit interaction into $^2F_{5/2}$ and $^2F_{7/2}$ and split further into Kramers doublets by the crystal-field interaction. The lobes of the wavefunctions of 5d electrons are expanded towards ligand ions, and the energy levels are strongly affected by the surrounding environment. The magnitude of the crystal-field splitting, $10Dq$, between the 5d energy levels is estimated to be roughly $12\,000\ \mathrm{cm}^{-1}$ for Ce^{3+} in $LiYbF_4$ from the separation between the absorption band energies [3]. In consequence, the crystal-field interaction for the excited state is expected to be much larger than the spin–orbit interaction. In S_4 symmetry, the excited 5d state is split into t_{2g} ($|xy\rangle, |yz\rangle, |zx\rangle$) and e_g ($|2z^2 - x^2 - y^2\rangle, |x^2 - y^2\rangle$). As the lobes of the wavefunctions $|xy\rangle, |yz\rangle, |zx\rangle$ are expanded towards F^- ligand ions as shown in figure 1, the t_{2g} excited state is higher in energy than the e_g excited state [3]. In a tetragonal distortion, the e_g excited state is expected to be split further into two levels, $|x^2 - y^2\rangle$ being lower, because the lobe of $|x^2 - y^2\rangle$ is expanded between four F^- ligands, up and down, close to the aa-(xy-) plane.

The polarization is determined by the optical transition probability calculated using the wavefunctions of the 4f ground and 5d excited states, which is parity allowed. If the lowest 5d excited state is pure $|x^2 - y^2\rangle$, the absorption to the excited state has only σ-polarization because the electron density of the wavefunction is localized in the xy-plane. In the same way, the π-polarization is dominant for the transition to $|2z^2 - x^2 - y^2\rangle$. This expectation can explain qualitatively the features of the polarizations. However, in order to explain the ratio of the π- and σ-polarization, the optical transition probabilities have to be calculated using realistic wavefunctions of the ground and excited states perturbed through both the crystal-field and spin–orbit interactions.

5. Conclusions

The g-tensor of the Ce^{3+} ESR spectra indicates that Ce^{3+} ions occupy the centre of a dodecahedron with a negative value of the crystal-field parameter B_2^0, which is consistent with the results obtained for Er^{3+} in $LiYF_4$. In consequence, $LiYF_4$ crystals are regarded as an ideal matrix for Ce^{3+} ions, which replace Y^{3+} ions without charge compensation. The polarization of the optical absorption spectra is explained in terms of the wavefunctions of the 5d excited state in such a tetragonal distortion.

Acknowledgments

At Strathclyde, this research programme was funded by joint EPSRC/MOD research grants (GR/F/54105 and GR/H/66143). In Japan, the work was supported by a Grant-in-Aid for Scientific Research on the Priority Area ‘New Development of Rare Earth Complexes’ (Nos 07230233, 08220228, 07650049) from The Ministry of Education, Science and Culture, and

by joint research (1995–1996) between the Japan Society for the Promotion of Science and the Royal Society/British Council. The authors would like to thank Dr Kindo, Osaka University, for providing us with the opportunity to measure the ESR spectra at low temperatures.

References

[1] Blasse G and Grabmaier B C 1994 *Luminescent Materials* (Berlin: Springer)
[2] Pedrini C, Bouttet D, Dujardin C, Belsky A and Vasil'ev A 1996 *Proc. Int. Conf. on Inorganic Scintillators and Their Applications, SCINT95* (Delft: Delft University Press) p 103
[3] Verweij J W M, Pedrini C, Bouttet D, Dujardin C, Lautesse H and Moine B 1995 *Opt. Mater.* **4** 575
[4] Moulton P 1985 *Laser Handbook* vol 5, ed M Bass and M H Stitch (Amsterdam: North-Holland) p 282
[5] Okada F, Togawa S and Ohta K 1994 *J. Appl. Phys.* **75** 49
[6] Gabbe M R and Harmer A L 1968 *J. Cryst. Growth* **3** 544
[7] Mims W B 1964 *Phys. Rev.* **133** A835
[8] Mims W B 1965 *Phys. Rev.* **140** A531
[9] Sattler J P and Nemarich J 1971 *Phys. Rev.* B **4** 1
[10] Orton J W 1968 *Electron Paramagnetic Resonance* (London: Iliffe) p 119
[11] Abragam A and Bleaney B 1970 *Electron Paramagnetic Resonance of Transition Ions* (Oxford: Clarendon) p 33
Abragam A and Bleaney B 1970 *Electron Paramagnetic Resonance of Transition Ions* (Oxford: Clarendon) ch 5
[12] Brown M R, Roots K G and Shand W A 1969 *J. Phys. C: Solid State Phys.* **2** 583
[13] Vishwamittar and Puri S P 1974 *J. Phys. C: Solid State Phys.* **7** 1337